



In chronic complete spinal cord injury supraspinal changes detected by quantitative MRI are confined to volume reduction in the caudal brainstem

Andreas Hug^{a,*}, Adriano Bernini^b, Haili Wang^a, Antoine Lutti^b, Johann M.E. Jende^d, Markus Böttinger^a, Marc-André Weber^{c,e}, Norbert Weidner^a, Simone Lang^a

^a Spinal Cord Injury Center, Heidelberg University Hospital, Heidelberg, Germany

^b Laboratory for Research in Neuroimaging (LREN), Department of Clinical Neurosciences Lausanne University Hospital, University of Lausanne, Lausanne, Switzerland

^c Department of Radiology, Heidelberg University Hospital, Heidelberg, Germany

^d Department of Neuroradiology, Heidelberg University Hospital, Heidelberg, Germany

^e Institute of Diagnostic and Interventional Radiology, University Medical Center Rostock, Rostock, Germany

ARTICLE INFO

Keywords:

Spinal cord injury
Structural MRI
Atrophy

ABSTRACT

There is much controversy about the potential impact of spinal cord injury (SCI) on brain anatomy and function, which is mirrored in the substantial divergence of findings between animal models and human imaging studies. Given recent advances in quantitative magnetic resonance imaging (MRI) we sought to tackle the unresolved question about the link between the presumed injury associated volume differences and underlying brain tissue property changes in a cohort of chronic complete SCI patients. Using the established computational anatomy methods of voxel-based morphometry (VBM) and voxel-based quantification (VBQ), we performed statistical analyses on grey and white matter volumes as well as on parameter maps indicative for myelin, iron, and free tissue water content in the brain of complete SCI patients ($n = 14$) and healthy individuals ($n = 14$). Our regionally unbiased white matter analysis showed a significant volume reduction of the dorsal aspect at the junction between the most rostral part of the spinal cord and the medulla oblongata consistent with Wallerian degeneration of proprioceptive axons in the dorsal column tracts in SCI subjects. This observation strongly correlated with spinal cord atrophy assessed by quantification of the spinal cord cross-sectional area at the cervical level C2/3. These findings suggest that Wallerian degeneration of the dorsal column tracts represents a main contributor to the observed spinal cord atrophy, which is highly consistent with preclinical histological evidence of remote changes in the central nervous system secondary to SCI. Structural changes in other brain regions representing remote changes in the course of chronic SCI could neither be confirmed by conventional VBM nor by VBQ analysis. Whether and how MRI based brain morphometry and brain tissue property analysis will inform clinical decision making and clinical trial outcomes in spinal cord medicine remains to be determined.

1. Introduction

Spinal cord injury (SCI) is a major cause of chronic disability and profoundly affects patients' autonomy and quality of life. Despite the abundance of empirical evidence on the local effects of SCI along the spinal cord, our understanding of the concomitant changes in brain structure and function is still limited. For the putative supraspinal structural changes, detection through *in vivo* methodology might help to explain different recovery courses of patients with initially similar clinical severity. Such measurable alterations could therefore have

prognostic value. Moreover, amelioration of structural brain changes following a therapeutic intervention (e.g. administration of cell transplants, biomaterials, soluble compounds) could serve as a biomarker, which would provide an objectively measurable treatment effect.

Animal SCI models showed controversial results on remote supraspinal structural changes of the central nervous system, ranging from extensive neuronal cell death in cortical areas (Hains et al., 2003) and the rubrospinal tract (Viscomi and Molinari, 2014) to the absence of upper motoneuron degeneration or cell death of corticospinal neurons (Nielson et al., 2010, 2011). The lack of in-depth knowledge about the

* Corresponding author at: Spinal Cord Injury Center, Heidelberg University Hospital, Schlierbacher Landstraße 200a, 69118 Heidelberg, Germany.
E-mail address: andreas.hug@med.uni-heidelberg.de (A. Hug).

<https://doi.org/10.1016/j.nicl.2021.102716>

Received 8 February 2021; Received in revised form 31 May 2021; Accepted 1 June 2021

Available online 10 June 2021

2213-1582/© 2021 The Author(s).

Published by Elsevier Inc.

This is an open access article under the CC BY-NC-ND license

(<http://creativecommons.org/licenses/by-nc-nd/4.0/>).

impact of SCI on brain anatomy in humans highlights the need to provide *in vivo* analytic proof of concomitant structural changes that could inform clinical decision-making concerning treatment and prognosis.

Computational anatomy methods using magnetic resonance imaging (MRI) and mathematical algorithms to extract relevant brain features allow for statistical analysis of volume, shape, and surface in three-dimensional brain space (Ashburner et al., 2003). MRI has the advantage to screen in a much more unbiased fashion - compared to much more targeted microscopy based preclinical investigations - a complete brain in respect to structural changes. The exact pathophysiological underpinning remains to be determined. In SCI, one of the well-established methods, voxel-based morphometry (VBM), was applied by several investigators to identify local grey matter structural changes. Varying results were reported, ranging from the lack of SCI-related brain anatomy changes (Crawley et al., 2004) to evidence of profound structural sensorimotor cortex reorganization (Jurkiewicz et al., 2006; Wrigley et al., 2009; Freund et al., 2011, 2013; Henderson et al., 2011; Grabher et al., 2015; Chen et al., 2017). Concerning the involved brain regions, more recent reports demonstrate grey matter loss even in non-sensorimotor areas including anterior cingulate gyrus, insula, orbito-frontal gyrus, prefrontal cortex, and thalamus (Wrigley et al., 2009; Grabher et al., 2015; Chen et al., 2017). One of the potential reasons for these heterogeneous findings might be the fact, that these studies pooled together patients with incomplete and complete SCI (Crawley et al., 2004; Jurkiewicz et al., 2006; Freund et al., 2011, 2013; Grabher et al., 2015; Chen et al., 2017) and not taking into account the potential impact of differences in the time since injury. The non-quantitative character of the used T1-weighted MRI protocols represents another source for differences between studies. The computer-based estimation of regional volumes and cortical thickness from T1-weighted data is heavily dependent on the MR contrast, which is influenced by local histological tissue properties that give potentially rise to spurious morphological changes (Lorio et al., 2016b).

Recent advances allow using relaxometry maps indicative for myelin (magnetization transfer saturation – MT), iron (transverse relaxation rate - $R2^*$), the combination between the two (longitudinal relaxation rate – $R1$) and tissue free water (proton density flat map – PD^*) in the framework of voxel-based quantification (VBQ). VBQ delivers statistical parametric maps in brain space that allow for inferences about corresponding brain tissue properties according to a bio-physical multi-compartment model (Helms et al., 2008; Draganski et al., 2011; Lutti et al., 2014). Longitudinal investigations over the first 12 months post-injury applying tensor based morphometry (TBM) restricted to a set of anatomical regions of interest (ROIs) such as the corticospinal tract showed progressive white matter volume loss in the internal capsule of SCI patients paralleled by reductions in MT and $R1$ in the same brain regions at 12 months post-injury (Freund et al., 2013). Using the same technique in the same cohort for different anatomical ROIs, the authors observed additional brain areas with reductions on myelin-sensitive parameter maps in the thalamus, cerebellum, and brainstem during the same period (Grabher et al., 2015). Of note, these parallelized structural (VBM) and microstructural (VBQ) changes in the early phase after SCI, contrast with the absence of volume differences when comparing sub-acute (duration <1 year) and chronic (duration >1 year) patients with complete motor SCI (Chen et al., 2017).

Here we sought to address previous uncertainties in the field and to investigate the sensitivity of quantitative MRI to detect structural brain changes secondary to SCI in a more homogenous cohort of chronic complete SCI subjects. We used established VBM and VBQ methods to study potential structural and microstructural differences associated with SCI. In a first unbiased hypothesis-free analytical approach we analyzed the total grey and white matter volumes unrestricted for anatomical ROIs. For secondary sensitivity analyses, we either restricted the model fit or the statistical analysis (small volume correction) to putatively relevant ROIs (i.e. bilateral primary motor cortex, corticospinal tract).

2. Materials and methods

2.1. Study participants

All study-related procedures were performed after obtaining informed consent according to protocols approved by the independent local ethics committee. We screened all patients admitted to the Spinal Cord Injury Center at Heidelberg University Hospital, Germany, for eligibility to participate in the study. The main inclusion criterion was sensorimotor complete spinal cord injury (American Spinal Injury Association Scale (AIS) grade A) that dated back at least 3 months before study entry. Clinical scoring and grading were done according to the International Standards for Neurological Classification of Spinal Cord Injury (ISNCSCI) (Kirshblum et al., 2011). The selection of control individuals aimed for the minimization of between-group differences of factors that are known to be associated with brain volume (i.e., age and sex) (Barnes et al., 2010).

2.2. MRI acquisition

All MRI data were acquired on a 3 Tesla scanner (Siemens Verio, Siemens Healthineers, Germany). We used the same MRI scanner throughout the duration of the study. Due to the cross-sectional experimental design with one scan per subject, geometry correction was not applicable. Patients and healthy controls were equally distributed along the timeline of the project, which should have minimized the probability of any time-related bias. The imaging protocol consisted of three whole-brain multi-echo 3D fast low angle shot (FLASH) acquisitions with magnetization transfer-weighted (MTw: $TR/\alpha = 24.5 \text{ ms}/6^\circ$), proton density-weighted (PDw: $TR/\alpha = 24.5 \text{ ms}/6^\circ$) and T1-weighted (T1w: $24.5 \text{ ms}/21^\circ$) sequences (Helms et al., 2009; Helms et al., 2008; Weiskopf et al., 2013). For each sequence, we acquired multiple gradient echoes with a minimum of 2.46 ms and equidistant 2.46 ms echo spacing. Per echo 176 sagittal partitions with 1 mm isotropic voxel size (field of view and matrix size 256×240) and alternating readout polarity were acquired. The number of echoes was 7/8/8 for the MTw/PDw/T1w sequences to keep the TR value identical for all sequences. We used parallel imaging along the phase-encoding direction (acceleration factor 2 with GRAPPA reconstruction) (Griswold et al., 2002) and partial Fourier imaging (factor 6/8) along the partition direction.

2.3. Map calculation

The $R2^*$, MT, PD^* , and $R1$ quantitative maps were calculated as previously described (Draganski et al., 2011). For map calculation, we used in-house software running under SPM12 (Wellcome Trust Centre for Neuroimaging, London, UK; www.fil.ion.ucl.ac.uk/spm) and Matlab R2020a (Mathworks, Sherborn, MA, USA). $R2^*$ maps were estimated from the regression of the log-signal of the eight PD-weighted echoes. MT and $R1$ maps were created using the MTw, PDw and T1w images averaged across all echoes (Helms et al., 2008). All maps were corrected for local radiofrequency (RF) transmit field inhomogeneities using the inhomogeneity correction UNICORT algorithm in the framework of SPM12 (Weiskopf et al., 2011).

2.4. Voxel-based morphometry (VBM) and voxel-based quantification (VBQ)

For automated tissue classification in grey matter (GM), white matter (WM), and cerebrospinal fluid (CSF) we used the MT maps within the SPM12 “unified segmentation” approach (Ashburner and Friston, 2005) with default settings and enhanced tissue probability maps (Lorio et al., 2016a) that provide optimal delineation of subcortical structures. Aiming at optimal anatomical precision, we estimated subject-specific spatial registration parameters using the diffeomorphic algorithm based on exponentiated lie algebra - DARTEL (Ashburner, 2007). For

VBM analysis, we scaled the probability maps with the corresponding Jacobian determinants to preserve the initial total amount of signal intensity. For VBQ analysis, we followed the same strategy by applying a weighted averaging procedure that ensures the preservation of the initial signal intensity of the MT, PD* and R2* parameter maps (Draganski et al., 2011). The resulting maps were spatially smoothed using an isotropic Gaussian convolution kernel of 8 mm full-width-at-half-maximum.

2.5. Spinal cord cross-sectional area (CSA) assessment

CSA assessment was performed on averaged T1w sequences in the axial plane using the software package snap-ITK (Yushkevich et al., 2006). Delineation of the spinal cord was performed by outlining the spinal cord circumference manually (AH) at the C2/3 level slice by slice in the axial plane yielding a total of 15 continuous slices. For an approximation of the mean CSA of the upper spinal cord, we averaged the CSA over these 15 slices.

2.6. Statistical analysis

We used parametric and nonparametric statistics from the software package JMP® - v15, for descriptive analysis of clinical data where deemed appropriate.

Sample size considerations: In SCI, absolute effect sizes have hardly been published in previous quantitative MRI research. The study by Freund et al. (2013) showed a reduction in volume one year after SCI at the capsula interna level of approx. 2%. The standard error of mean (SE) was approx. 0.5%. The study included $n = 12$ patients. According to the formula $SD = SE \times \sqrt{N}$ the standard deviation (SD) in the SCI group is 1.8. Under the Normality assumption, using t -test means with an allocation 1:1, an estimated α error probability of 0.05 and a power (1- β error probability) of 0.8 a total of about 28 subjects ($n = 14$ per group) would be required (Faul et al., 2007).

In a first regionally unbiased statistical attempt, a voxel-wise general linear model (GLM) was fitted to the total grey and white volumes, respectively. This was done separately for each parameter map (VBM, MT, PD*, R1, R2*). Regressors in the final model were the categorical group indicator variable (SCI versus control), age, sex, and total intracranial volume (Barnes et al., 2010). Total intracranial volume was calculated as the sum of the segmented grey matter, white matter, and CSF volumes from MTw images. Model parameterization was done applying an independent two-sample t -test design as implemented in SPM12. After model estimation, the group effect was analyzed by an unbiased two-sided F-contrast statement for the total volumes (without small volume corrections for anatomical ROIs). Thereafter, one-sided T-contrast statements were used to analyze the direction of the identified differences (i.e. reductions or increases of volume (VBM) and intensities (VBQ), respectively). To control for multiple comparisons in this mass-univariate voxel-wise analysis, family-wise error (FWE) correction methods using Random Field Theory were applied. The peak level height threshold for statistical significance was set at FWE $p < 0.05$ with no cluster extent threshold.

In additional sensitivity analyses in analogy to a previous study (Freund et al., 2013), we also fitted the model to restricted anatomical regions of interest (ROIs) consisting of the bilateral primary motor cortex (grey matter) and corticospinal tracts (white matter), respectively. Further sensitivity analyses consisted of small volume corrections for these anatomical ROIs during statistical inference after fitting the model to the whole grey or white matter volumes.

Because of the strong association between spinal cord CSA and group membership (SCI, control), additional voxel-wise statistical models were fitted to assess correlations between brain volume changes and spinal cord CSA. The final models consisted of the regressors: CSA, age, sex, and total intracranial volume. Model parameterization was done applying a multiple regression design as implemented in SPM12.

To obtain the effect size of significant voxel-wise correlations

Table 1

Characteristics of SCI and control subjects. AIS (American Spinal Injury Association Impairment Scale), NLI (Neurological Level of Injury).

ID	Age (years)	AIS	NLI	Time since injury (months)
P1	66	A	C7	531
P2	62	A	T7	519
P3	32	A	T10	206
P4	59	A	T5	122
P5	55	A	T3	114
P17	21	A	C5	7
P19	59	A	T5	4
P20	65	A	T8	4
P21	61	A	T6	66
P22	53	A	C6	16
P25	52	A	C3	385
P30	65	A	C6	568
P32	62	A	T9	567
P34	58	A	T5	165
C2	27			
C3	24			
C7	52			
C8	39			
C9	50			
C12	61			
C14	69			
C15	38			
C16	64			
C18	28			
C26	50			
C27	25			
C28	63			
C31	55			

between brain volume and spinal cord CSA or the group status, separate analyses were performed outside the SPM12 framework after extraction of the values in significant brain clusters. For illustration purposes MRICronGL 1.2.20201102 obtained from www.nitrc.org was used.

3. Results

3.1. Population characteristics

MRI scans were obtained during a sampling period of 3.5 years. The main clinical characteristics of the patient population are summarized in TABLE 1. We recruited 14 patients and 14 control subjects. The mean age in the control and patient group was 46 ± 16 and 55 ± 13 years ($p = 0.1147$), respectively. The female to male ratio was 3:11 in each group. The median time since SCI was 144 (4–568) months. Lesion severity in all patients was sensorimotor complete (AIS grade A). The TIV in the healthy control cohort was 1571 ± 171 ml (mean \pm SD) and 1479 ± 210 ml in SCI subjects ($p = 0.2169$).

3.2. VBM and VBQ analysis

In regionally unbiased VBM analysis, we observed WM volume reductions in the dorsal aspect at the junction between the most rostral part of the spinal cord and the medulla oblongata (MNI coordinates: -1.5 – 48 -67.5) in SCI subjects compared to healthy controls (mean difference \pm SEM: 11.7 ± 1.9 μ l) (Fig. 1). We could not observe any other significant grey or white matter brain volume differences. Unbiased VBQ analysis did not reveal any significant between-group differences.

Sensitivity analyses restricted to anatomical region of interest confirmed the volume reductions in the medulla oblongata of SCI patients. Moreover, these ROI analyses confirmed the absence of any other between-group differences. For a summary of these results at the uncorrected $p = 0.001$ level see supplementary Table 1.

The cross-sectional area (CSA) analysis at the cervical level revealed smaller CSA in SCI subjects compared to controls (60.2 ± 8.1 mm^2 versus 74.5 ± 10.4 , $p < 0.001$). We found a strong positive correlation

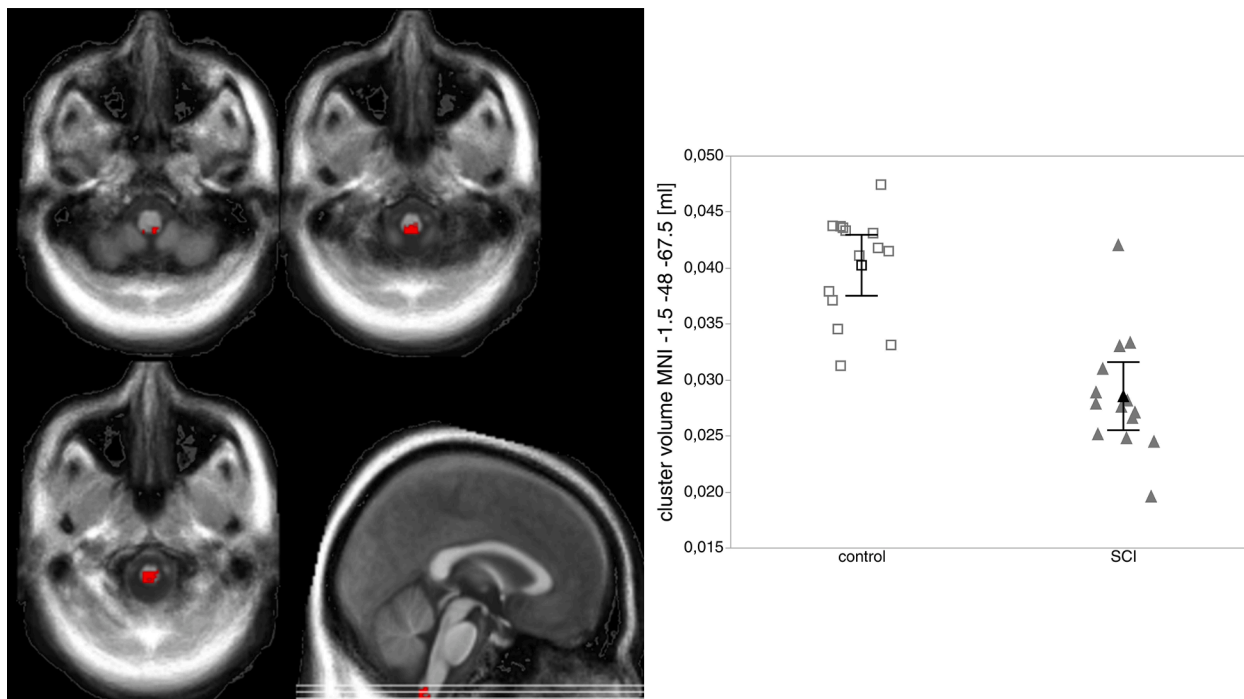


Fig. 1. Left panel: color-coded voxels depict reduced WM volume in the dorsal aspect at the junction between the most rostral part of the spinal cord and the medulla oblongata (statistical FWE-peak voxel at MNI coordinates: $-1.5-48 -67.5$) in SCI subjects compared to healthy control individuals. The color scale represents T-values (model fit and statistics apply to the total white matter volume; peak $T = 5.82$, $p = 0.014$ FWE). For illustration purposes, representative axial slices with significant voxels in VBM analysis at the $\alpha < 0.001$ uncorrected statistical threshold level were used. The structural image was calculated as the mean R1 image of the study sample after running the DARTEL algorithm. Right panel: To illustrate the effect size in the significant cluster at MNI $-1.5-48 -67.5$ absolute volumes of that cluster were calculated for each study subject (open rectangles for controls, closed triangles for SCI). Symbols with errorbars represent the group mean $\pm 2xSEM$. The mean difference $\pm SEM$ between groups was $11.7 \pm 1.9 \mu l$.

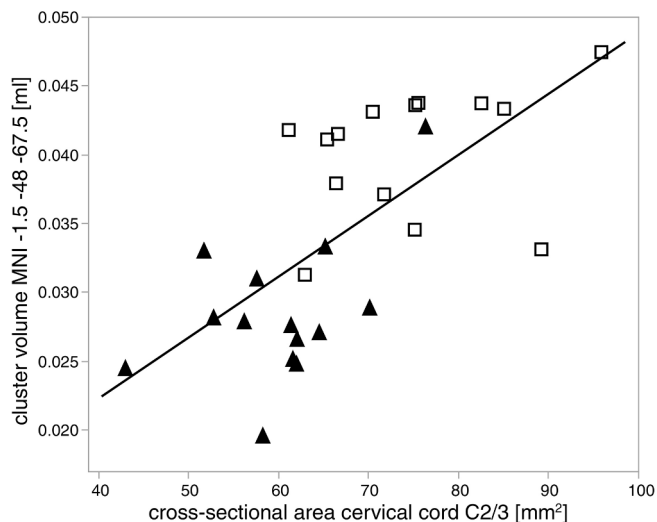


Fig. 2. Strong positive correlation between the medulla oblongata cluster with reduced volume at MNI $-1.5-48 -67.5$ and the cross-sectional area at the spinal level C2/3 ($r = 0.662$; $p < 0.001$). Symbols indicate the groups: SCI-patients (filled triangles), healthy controls (open rectangles).

between the loss of cervical level CSA and WM volume at MNI $-1.5-48 -67.5$ ($r = 0.662$; $p < 0.001$; Fig. 2). CSA was not associated with any other WM or GM brain volume change, respectively.

4. Discussion

In this study, we identified WM volume loss (approximately $11 \mu l$) in

the dorsal aspect at the junction between the most rostral part of the spinal cord and the medulla oblongata in chronic sensorimotor complete SCI subjects. This volume loss correlated with spinal cord atrophy at the cervical level. In contrast to published results, despite a reasonable sample size with higher homogeneity from a clinical and pathophysiological point of view, we were not able to find any other structural differences in SCI patients that reached the accepted levels of statistical significance.

The highest impact in respect to changes remote from the injury site can be expected from a long duration since injury together with complete axon transection in long descending/ascending tracts (reflected by a sensorimotor complete SCI), which have the highest potential to (1) induce retrograde axon degeneration, demyelination and neuronal cell death (in case these pathophysiological events really occur) and/or (2) cause maximum Wallerian degeneration of long ascending sensory projections, demyelination and transsynaptic degeneration. Based on these criteria, the characteristics of our study cohort with a median time since SCI of 144 months and an average injury completeness of 95.4% (total motor score loss in relation to the achievable total motor score under consideration of the lesion level) are well suited to induce substantial supraspinal changes.

The reduced volume in the dorsal aspect at the junction between the most rostral part of the spinal cord and the medulla oblongata in SCI subjects most likely reflects Wallerian degeneration of large proprioceptive sensory axons, which has been established histologically (Becerra et al., 1995; Weber et al., 2006). It is unlikely that the identified volume reduction in this area was generated by a software algorithm induced imaging artifact due to false classification/registration (Bookstein, 2001). Quality inspection of the normalized images after application of the DARTEL algorithm did not indicate false classification or registration. Methodologically, volume changes in similar regions could be shown earlier for other neurological diseases such as Parkinson's

Table 2
Comprehensive overview of the individual studies.

First Author	Crawley	Jurkiewicz	Wrigley	Freund	Henderson	Freund	Grabher	Chen	Hug
sample similarity	1	1	2	3	2	4	4	5	6
Pub year	2004	2006	2009	2011	2011	2013	2015	2017	2021
PMID	15,518,637	16,534,122	18,483,004	21,586,596	21,325,531	23,827,394	26,290,444	28,503,142	
Raw data sequence	T1w	T1w	T1w	T1w(MDEFT)	T1w	T1w	T1w	T1w	MPM
Scanner	Signa	Signa	Achieva	Sonata	Intera	Verio	Verio	Trio Tim	Verio
Field strength	1.5 T	1.5 T	3.0 T	1.5 T	3.0 T	3.0 T	3.0 T	3.0 T	3.0 T
Segmentation method	manual	VBM (SPM2)	VBM (SPM5) unified segmentation	VBM (SPM8) unified segmentation	VBM (SPM5) unified segmentation	TBM (SPM12) VBM (SPM12) VBQ (SPM12) unified segmentation	TBM (SPM12) VBQ (SPM12) unified segmentation	VBM (SPM8) unified segmentation	VBM(SPM12) VBQ (SPM12) unified segmentation
Modulation	yes	yes	yes	yes	yes	yes	yes	yes	yes
Normalisation Model	Standard ANCOVA	Standard ANCOVA	Standard ANCOVA	DARTEL ANCOVA	Standard ?	DARTEL ?	DARTEL ?	DARTEL T-test	DARTEL T-test
Model covariates (nuisance)	global GM	global GM	age	age	age sex	age TIV	age TIV	age sex	age sex TIV
Multiple comparison correction	?	?	FDR 0.05	FWE 0.05	?	FWE 0.05	FWE 0.05	FWE 0.05	FWE 0.05
ROI	M1 global WM	S1 M1 global WM	?	Whole-Brain M1 S1hand S1leg CST	S1	M1 S1 CST	ACC Thalamus S1 S2 insula cerebellum brainstem	global GM sig clusters (for subgroups)	global GM global WM M1 CST
SVC	?	?	?	10 mm sphere	?	?	?	?	without and anatomical ROI (CST, M1)
VBM sign. regions	none	S1_r S1_l	M1_l mPFC_r mPFC_l ACC_r ACC_l TEMP_r TEMP_l Hypo Insula	Pyramids_rl CerebellarPed_l M1_r S1_r	S1_r S1_l	M1_l CST_l	VBM: not done TBM: Thalamus_r Thalamus_l ACC_r ACC_l Insula_l S2_l Pons	ACC_r OFC_r OFC_l Insula_r Insula_l TEMP_r	global GM spinal cord
Effect size SCI-con	n.a.	-25 ± 4% -18 ± 4%	?	?	0.33 ± 0.02-0.45 ± 0.05 0.26 ± 0.03-0.39 ± 0.07	TBM: approx. -2% VBM: not done	TBM: up to approx. -3%	0.5 ± 0.05-0.6 ± 0.05	-11.7 ± 1.9 µl
VBQ sign. regions	not done	not done	not done	not done	not done	R1: M1_rl S1_rl CST_rl MT: M1_rl S1_rl CST_r	R1: Thalamus_rl Cerebellum_r M1: Medulla	not done	none
Effect size SCI-con	n.a.	n.a.	n.a.	n.a.	n.a.	not done	-19% -17% -14%	n.a.	n.a.
n (SCI)	17	17	15	10	20	13	14	21	14
n (controls)	16	16	27	16	23	18	18	21	14
NLI	C3-S1	C3-S1	T1-T10	C5-C8	T1-T10	C4-T12	C4-T12	C3-Sn	C3-T10
T:P	16:1	16:1	0:15	10:0	0:20	8:5	8:6	8:13	5:9
AIS	A-11 B-3 D-2 E-1	A-11 B-3 D-2 E-1	A-15	A-2 B-1 C-3 D-4	A-20	A-4 B-5 D-4	A-5 B-5 D-4	A-10 B-1 C-2 D-8	A-14
Duration	1-160	1-160	24-390	84-360	24-444	12	12	1-396	4-568
Age	21-54	21-54	26-57	29-61	22-57	19-75	19-75	28-71	21-66
m:f (SCI)	13:4	13:4	15:0	10:0	18:2	12:1	13:1	15:6	11:3
m:f (con)	8:8	8:8	27:0	?	20:3	12:6	12:6	15:6	11:3

ACC: anterior cingulate cortex; AIS: American Spinal Injury Association Impairment Scale Grade; ANCOVA: analysis of covariance; CerebellarPed: cerebellar peduncle; con: control; CST: corticospinal tract; DTI: diffusion tensor imaging; f: female; FDR: false discovery rate; FWE: family-wise error; GM: grey matter; M1: primary motor cortex; m: male; MDEFT: Modified Driven Equilibrium Fourier Transform; MPM: multiparameter mapping allowing VBM and VBQ analyses; n.a.: not applicable; NLI: neurological level of injury; OFC: orbitofrontal cortex; P: paraplegic; PMID: PubMed identifier; Pub year: year of publication; ROI: region of interest; S1: primary somatosensory cortex; S2: secondary somatosensory cortex; Sample similarity: studies with largely similar cohorts have identical numbers; SCI: spinal cord injury;

sign.: significant; SPM: statistical parametric mapping; suffix_l: left; suffix_r: right; suffix_rl: both sides; SVC: small volume correction; T: tetraplegic; TBM: tensor based morphometry; TEMP: temporal cortex; TIV: total intracranial volume; VBM: voxel based morphometry; VBQ: voxel based quantification; WM: white matter

disease (Jubault et al., 2009). The strong positive correlation between the spinal cord cross-sectional area at the C2/3 level and the identified WM volume cluster at the spinal cord-medulla oblongata junction also supports our hypothesis of a true biological effect. Atrophy at the cervical cord and medulla oblongata level is a consistent finding after SCI, which is associated with more severe disability (Freund et al., 2010, 2011, 2013).

WM volume reductions in the brain stem, topographically related to the corticospinal tracts and in the left cerebellar peduncle, have been previously reported in a clinically more heterogeneous (more incomplete SCI subjects) and a less chronic cohort of SCI subjects (Freund et al., 2011, 2013). However, volume changes in respective neuroanatomical regions could not be reproduced in our chronic sensorimotor complete SCI cohort. The volume reductions in our cohort were located more dorsal and caudal between the spinal cord and medulla oblongata consistent with the neuroanatomical region of the dorsal funiculus. Whether degenerative changes such as retrograde axon dieback or neuronal atrophy/cell death occur in corticospinal projections as suggested by VBM/VBQ studies (Freund et al., 2011, 2013) is still debated. Recent preclinical studies indicate that neuronal cell death as a consequence of corticospinal tract transection – at least in rodents – cannot be observed (Nielson et al., 2010, 2011). However, a mild reduction in cell size 4 weeks after a thoracic dorsal column transection in rats was detected. This finding could represent the pathophysiological basis of gray matter volume changes detected with VBM within the first year after injury in human subjects (Freund et al., 2013). However, it is unknown whether these cell size changes as observed in rodents are only transient and do not reflect an irreversible state (“progressive atrophy”) as suggested (Freund et al., 2019). It is conceivable that changes within the brain detected by VBM (Freund et al., 2013) reflect transient volume changes as previously shown (Draganski et al., 2004), which disappear/normalize over longer periods of time. This would explain the absence of structural changes in our chronic SCI cohort. Recent evidence directly comparing VBM with advanced microscopy techniques (Asan et al., 2021) in mice suggests that “gray matter volume changes are not strongly related to changes in physical volume”. Rather “local cell count, spatial arrangement of cells as well as cell type composition are factors that make important contributions.” Accordingly, it appears less likely that cell size changes (Nielson et al., 2011) identified microscopically represent the correlate of VBM based volume changes. Remote changes in the brain related to neurogenesis or gliogenesis, which also could have produced volumetric changes in VBM studies (Killgore et al., 2013), could not be observed in animal models of SCI (Franz et al., 2014). Post-mortem histological data from human SCI subjects are not available to either confirm or reject such changes.

Differences in supraspinal VBQ parameter maps, which are supposed to reflect microstructural alterations associated with myelin (MT and R1), could not be observed in our study. This contrasts previous findings of reductions of MT and R1 in brains of SCI subjects within the first year after injury (Freund et al., 2013). We are not aware of any animal or human study, which has shown demyelination in the brain as a consequence of spinal cord injury.

Regarding the involved brain regions in SCI subjects, previous morphometric MRI studies reported diverse findings (Crawley et al., 2004; Jurkiewicz et al., 2006; Wrigley et al., 2009; Freund et al., 2011, 2013; Chen et al., 2017). In our current study on chronic sensorimotor complete SCI, we were not able to unambiguously identify any other brain or brainstem region associated with VBM or VBQ changes. Of note, our sensitivity analyses on putatively involved anatomical ROIs (i.e. bilateral primary motor cortex and corticospinal tracts) also did not unmask any other VBM or VBQ changes in SCI subjects.

Concerning the sample homogeneity of clinically relevant parameters among the investigated SCI group, only one other group (Wrigley

et al., 2009; Henderson et al., 2011) analyzed a comparably standardized population. However, our results do not support their finding of extensively reduced GM volumes in motor and non-motor regions of the brain associated with SCI.

Lack of statistical power is unlikely to explain the deviating findings. A clinically highly homogenous sample of 14 SCI subjects was investigated in the present study, whereas 10 (Freund et al., 2011), 13 (Freund et al., 2013), 15 (Wrigley et al., 2009), and 17 (Jurkiewicz et al., 2006) SCI subjects with a variable degree of clinical heterogeneity (i.e. complete/incomplete lesions, acute/chronic stages) were enrolled in previous MRI studies. Freund et al. (Freund et al., 2013) found a linear decrease in brain volume over a one-year period after SCI. In an attempt to maximize the signal to noise ratio by our experimental design, we therefore opted for the preferential inclusion of chronically paralyzed patients with long-lasting SCI. Nevertheless, we also included sub-acute patients within 6 months after injury according to the definition of the EMSCI-Project (emsci.org). However, we could not find a correlation in our data set between the duration of SCI and brain changes, which is consistent with previous research (Wrigley et al., 2009). It should be noted that the variable duration of SCI is not normally distributed. In this respect, modeling in statistical models is not straightforward.

Since image acquisition and post processing methods were identical in our study and the study by Freund et al. (Freund et al., 2013) differential appreciation of known confounding factors related to the study cohorts could explain contradictory findings. After normalization, men have been demonstrated to have smaller brain volumes than women (Barnes et al., 2010). However, the study by Freund et al. (Freund et al., 2013) failed to consider sex as a known confounder of brain volume, illustrated by an unbalanced design in respect to the male to female ratio (12:1 in SCI subjects versus 12:6 in controls subjects). In our study the respective ratio was 11:3, both, in the SCI group and the control group. The established substantial interactions of sex and brain morphometry constitutes in our opinion a significant bias in the Freund et al. study (Freund et al., 2013), since all variables (age, TIV, and sex) need to be considered in VBM studies (Barnes et al., 2010). Moreover, due to the potential non-linear interactions between sex and brain morphometry, such a bias cannot easily be adjusted for in linear statistical models implemented in SPM12.

For a more comprehensive overview of the individual studies, please refer to Table 2.

In summary, our VBM and VBQ analyses in a homogenous sample of chronic sensorimotor complete SCI subjects failed to detect structural or microstructural brain changes cranially to the medulla oblongata level attributable to SCI. These findings are supported by the absence of secondary neurodegenerative remote changes in the brain reported in preclinical animal studies. Furthermore, our SCI-specific finding of reduced cross-sectional areas in the upper cervical spinal cord, which is strongly associated with white matter volume loss at the junction between the cervical cord and medulla oblongata, is concordant with previous preclinical histological evidence of well-established remote changes after SCI. Consequently, applying the MRI methodology used in the current study, it is not unequivocally possible to detect suitable and clinically meaningful SCI-specific markers in the brain, which could help to facilitate clinical decision making or enrich innovative clinical trial designs.

Declaration of Competing Interest

The authors declare that they have no known competing financial interests or personal relationships that could have appeared to influence the work reported in this paper.

Acknowledgements

This study was supported by grants from the Deutsche Forschungsgemeinschaft (SFB1158) to Norbert Weidner and from the Medical Faculty Heidelberg to Andreas Hug. We acknowledge financial support by the Open Access Publishing Fund of Ruprecht-Karls-Universität Heidelberg. We thank Bogdan Draganski from the Department of Clinical Neurosciences Lausanne University Hospital, University of Lausanne, Switzerland, for his expert advice.

Appendix A. Supplementary data

Supplementary data to this article can be found online at <https://doi.org/10.1016/j.nicl.2021.102716>.

References

- Asan, L., Falfán-Melgoza, C., Beretta, C.A., Sack, M., Zheng, L., Weber-Fahr, W., Kuner, T., Knabbe, J., 2021. Cellular correlates of gray matter volume changes in magnetic resonance morphometry identified by two-photon microscopy. *Sci. Rep.* 11 (1) <https://doi.org/10.1038/s41598-021-83491-8>.
- Ashburner, J., 2007. A fast diffeomorphic image registration algorithm. *Neuroimage* 38 (1), 95–113.
- Ashburner, J., Csernansky, J.G., Davatzikos, C., Fox, N.C., Frisoni, G.B., Thompson, P.M., 2003. Computer-assisted imaging to assess brain structure in healthy and diseased brains. *Lancet Neurol.* 2 (2), 79–88.
- Ashburner, J., Friston, K.J., 2005. Unified segmentation. *Neuroimage* 26 (3), 839–851.
- Barnes, J., Ridgway, G.R., Bartlett, J., Henley, S.M.D., Lehmann, M., Hobbs, N., Clarkson, M.J., MacManus, D.G., Ourselin, S., Fox, N.C., 2010. Head size, age and gender adjustment in MRI studies: a necessary nuisance? *Neuroimage* 53 (4), 1244–1255.
- Becerra, J.L., Puckett, W.R., Hiester, E.D., Quencer, R.M., Marcillo, A.E., Post, M.J., et al., 1995. MR-pathologic comparisons of wallerian degeneration in spinal cord injury. *AJNR Am. J. Neuroradiol.* 16 (1), 125–133.
- Bookstein, F.L., 2001. “Voxel-based morphometry” should not be used with imperfectly registered images. *Neuroimage* 14 (6), 1454–1462.
- Chen, Q., Zheng, W., Chen, X., Wan, L., Qin, W., Qi, Z., Chen, N., Li, K., 2017. Brain gray matter atrophy after spinal cord injury: a voxel-based morphometry study. *Front. Hum. Neurosci.* 11, 211.
- Crawley, A.P., Jurkiewicz, M.T., Yim, A., Heyn, S., Verrier, M.C., Fehlings, M.G., Mikulis, D.J., 2004. Absence of localized grey matter volume changes in the motor cortex following spinal cord injury. *Brain Res* 1028 (1), 19–25.
- Draganski, B., Ashburner, J., Hutton, C., Kherif, F., Frackowiak, R.S.J., Helms, G., Weiskopf, N., 2011. Regional specificity of MRI contrast parameter changes in normal ageing revealed by voxel-based quantification (VBQ). *Neuroimage* 55 (4), 1423–1434.
- Draganski, B., Gaser, C., Busch, V., Schuierer, G., Bogdahn, U., May, A., 2004. Neuroplasticity: changes in grey matter induced by training. *Nature* 427 (6972), 311–312.
- Draganski, B., Frackowiak, R., Ashburner, J., Weiskopf, N., 2009. Improved segmentation of deep brain grey matter structures using magnetization transfer (MT) parameter maps. *Neuroimage* 47, 194–198.
- Faul, F., Erdfelder, E., Lang, A.-G., Buchner, A., 2007. G*Power 3: a flexible statistical power analysis program for the social, behavioral, and biomedical sciences. *Behav. Res. Methods* 39 (2), 175–191.
- Franz, S., Ciatipis, M., Pfeifer, K., Kierdorf, B., Sandner, B., Bogdahn, U., Blesch, A., Winner, B., Weidner, N., Di Giovanni, S., 2014. Thoracic rat spinal cord contusion injury induces remote spinal gliogenesis but not neurogenesis or gliogenesis in the brain. *PLoS ONE* 9 (7), e102896.
- Freund, P., Seif, M., Weiskopf, N., Friston, K., Fehlings, M.G., Thompson, A.J., Curt, A., 2019. MRI in traumatic spinal cord injury: from clinical assessment to neuroimaging biomarkers. *Lancet Neurol.* 18 (12), 1123–1135.
- Freund, P., Weiskopf, N., Ashburner, J., Wolf, K., Sutter, R., Altmann, D.R., Friston, K., Thompson, A., Curt, A., 2013. MRI investigation of the sensorimotor cortex and the corticospinal tract after acute spinal cord injury: a prospective longitudinal study. *Lancet Neurol.* 12 (9), 873–881.
- Freund, P., Weiskopf, N., Ward, N.S., Hutton, C., Gall, A., Ciccarelli, O., et al., 2011. Disability, atrophy and cortical reorganization following spinal cord injury. *Brain J. Neurol.* 134 (Pt 6), 1610–1622.
- Freund, P.A.B., Dalton, C., Wheeler-Kingshott, C.A.M., Glemsan, J., Bradbury, D., Thompson, A.J., Weiskopf, N., 2010. Method for simultaneous voxel-based morphometry of the brain and cervical spinal cord area measurements using 3D-MDEFT. *J. Magn. Reson. Imaging* 32 (5), 1242–1247.
- Grabher, P., Callaghan, M.F., Ashburner, J., Weiskopf, N., Thompson, A.J., Curt, A., Freund, P., 2015. Tracking sensory system atrophy and outcome prediction in spinal cord injury. *Ann. Neurol.* 78 (5), 751–761.
- Griswold, M.A., Jakob, P.M., Heidemann, R.M., Nittka, M., Jellus, V., Wang, J., Kiefer, B., Haase, A., 2002. Generalized autocalibrating partially parallel acquisitions (GRAPPA). *Magn. Reson. Med.* 47 (6), 1202–1210.
- Hains, B.C., Black, J.A., Waxman, S.G., 2003. Primary cortical motor neurons undergo apoptosis after axotomizing spinal cord injury. *J. Comp. Neurol.* 462 (3), 328–341.
- Helms, G., Dathe, H., Kallenberg, K., Dechent, P., 2008. High-resolution maps of magnetization transfer with inherent correction for RF inhomogeneity and T1 relaxation obtained from 3D FLASH MRI. *Magn. Reson. Med.* 60 (6), 1396–1407.
- Henderson, L.A., Gustin, S.M., Macey, P.M., Wrigley, P.J., Siddall, P.J., 2011. Functional reorganization of the brain in humans following spinal cord injury: evidence for underlying changes in cortical anatomy. *J. Neurosci.* 31 (7), 2630–2637.
- Jubault, T., Brambati, S.M., Degroot, C., Kullmann, B., Strafella, A.P., Lafontaine, A.-L., Chouinard, S., Monchi, O., Gendelman, H.E., 2009. Regional brain stem atrophy in idiopathic Parkinson’s disease detected by anatomical MRI. *PLoS ONE* 4 (12), e8247.
- Jurkiewicz, M.T., Crawley, A.P., Verrier, M.C., Fehlings, M.G., Mikulis, D.J., 2006. Somatosensory cortical atrophy after spinal cord injury: a voxel-based morphometry study. *Neurology* 66 (5), 762–764.
- Killgore, W.D., Olson, E.A., Weber, M., 2013. Physical exercise habits correlate with gray matter volume of the hippocampus in healthy adult humans. *Sci. Rep.* 3, 3457.
- Kirshblum, S.C., Waring, W., Biering-Sorensen, F., Burns, S.P., Johansen, M., Schmidt-Read, M., Donovan, W., Graves, D.E., Jha, A., Jones, L., Mulcahey, M.J., Krassioukov, A., 2011. Reference for the 2011 revision of the International Standards for Neurological Classification of Spinal Cord Injury. *J. Spinal Cord Med* 34 (6), 547–554.
- Lorio, S., Feresat, S., Adaszewski, S., Kherif, F., Chowdhury, R., Frackowiak, R.S., Ashburner, J., Helms, G., Weiskopf, N., Lutti, A., Draganski, B., 2016a. New tissue priors for improved automated classification of subcortical brain structures on MRI. *Neuroimage* 130, 157–166.
- Lorio, S., Kherif, F., Ruef, A., Melie-Garcia, L., Frackowiak, R., Ashburner, J., Helms, G., Lutti, A., Draganski, B., 2016b. Neurobiological origin of spurious brain morphological changes: a quantitative MRI study. *Hum Brain Mapp* 37 (5), 1801–1815.
- Lutti, A., Dick, F., Sereno, M.I., Weiskopf, N., 2014. Using high-resolution quantitative mapping of R1 as an index of cortical myelination. *Neuroimage* 93 (Pt 2), 176–188.
- Nielson, J.L., Sears-Kraxberger, I., Strong, M.K., Wong, J.K., Willenberg, R., Steward, O., 2010. Unexpected survival of neurons of origin of the pyramidal tract after spinal cord injury. *J. Neurosci.* 30 (34), 11516–11528.
- Nielson, J.L., Strong, M.K., Steward, O., 2011. A reassessment of whether cortical motor neurons die following spinal cord injury. *J. Comp. Neurol.* 519 (14), 2852–2869.
- Viscomi, M.T., Molinari, M., 2014. Remote neurodegeneration: multiple actors for one play. *Mol. Neurobiol.* 50 (2), 368–389.
- Weiskopf, N., Suckling, J., Williams, G., Correia, M.M., Inkster, B., Tait, R., Ooi, C., Bullmore, E.T., Lutti, A., 2013. Quantitative multi-parameter mapping of R1, PD(*), MT, and R2(*) at 3T: a multi-center validation. *Front Neurosci* 7, 95.
- Weber, T., Vroemen, M., Behr, V., Neuberger, T., Jakob, P., Haase, A., et al., 2006. Vivo high-resolution MR imaging of neuropathologic changes in the injured rat spinal cord. *Am. J. Neuroradiol.* 27 (3), 598–604.
- Weiskopf, N., Lutti, A., Helms, G., Novak, M., Ashburner, J., Hutton, C., 2011. Unified segmentation based correction of R1 brain maps for RF transmit field inhomogeneities (UNICORT). *Neuroimage* 54 (3), 2116–2124.
- Wrigley, P.J., Gustin, S.M., Macey, P.M., Nash, P.G., Gandevia, S.C., Macefield, V.G., Siddall, P.J., Henderson, L.A., 2009. Anatomical changes in human motor cortex and motor pathways following complete thoracic spinal cord injury. *Cereb. Cortex* 19 (1), 224–232.
- Yushkevich, P.A., Piven, J., Hazlett, H.C., Smith, R.G., Ho, S., Gee, J.C., Gerig, G., 2006. User-guided 3D active contour segmentation of anatomical structures: significantly improved efficiency and reliability. *Neuroimage* 31 (3), 1116–1128.